Linear Collider Collaboration Tech Notes

On Some Beam Dynamics Issues of NLC

September 8, 1999

J. Gao
LAL D'Orsay
Paris, France

Abstract:
In this report the single bunch and the multibunch dynamics are investigated analytically in the S-band, X-band linacs and IP regions. The relations between linac structure misalignments and the single bunch emittance growths are given. The relation between dipole mode quality factors vs. the wakefield reduction factors (one bunch separation) are found analytically for both linacs in order to prevent multibunch instabilities. Some preliminary discussions are given on the HOM coupler design for the S-band structure. As far as IP region is concerned, a special cavity is used to simulate the IP region, and it is found that the single bunch transverse deflection due to the short-range wakefield in this region is significant compared to the nominal vertical bunch size at the IP.

On Some Beam Dynamics Issues of NLC

J. Gao
SLAC, Stanford University, P.O. Box 4349, USA
and
Laboratoire de L'Accélérateur Linéaire
IN2P3-CNRS et Université de Paris-Sud
B.P. 34, F-91898 Orsay cedex, France

Abstract

In this report the single bunch and the multi-bunch dynamics are investigated in the S-band, X-band linacs and IP regions analytically. The relations between linac structure misalignments and the single bunch emittance growths are given. The relation between dipole mode quality factors vs the wakefield reduction factors (one bunch seperation) are found analytically for both linacs in order to prevent muti-bunch instabilities, and some preliminary discussions on the HOM coupler design for the S-band structure are given. As far as IP region is concerned, a spectial cavity is used to simulate IP region, and it is found that the single bunch transverse deflection due to the short range wakefield in this region is significant compared to the vertical norminal bunch size at IP.

1 Introduction

In this report we will discuss some beam dynamics issues in the linacs and the IP region of NLC. In section 2 single bunch emittance blow up in both S-band and X-band linacs are discussed. In section 3 we discuss multi-bunch transverse instability thresholds in both linacs. In section 4 the S-band HOM coupler design is briefly discussed. Finally, In section 5 the beam dynamics in IP region is investigated. To start with, we remind the reader that all the wakefields used in this report have been calculated by the formulae corresponding to a disk-loaded structure as shown in Fig. 1 [1].

The delta wakefield functions of a point charge traversing a disk-loaded structure can be calculated by using the following formulae:

$$W_z(\tau) = \sum_{m=0}^{\infty}\sum_{n=1}^{\infty}\sum_{l=0}^{\infty} W_{z,mnl}(\tau) \tag{1}$$

$$W_r(\tau) = \sum_{m=0}^{\infty}\sum_{n=1}^{\infty}\sum_{l=0}^{\infty} W_{r,mnl}(\tau) \tag{2}$$

$$W_\phi(\tau) = \sum_{m=0}^{\infty}\sum_{n=1}^{\infty}\sum_{l=0}^{\infty} W_{\phi,mnl}(\tau) \tag{3}$$

where

$$W_{z,mnl}(\tau) = 2k_{mnl}\left(\frac{r}{a}\right)^m\left(\frac{r_q}{a}\right)^m\cos(m\phi)\cos(\omega_{mnl}\tau) \tag{4}$$

$$W_{r,mnl}(\tau) = 2m\frac{ck_{mnl}}{\omega_{mnl}a}\left(\frac{r}{a}\right)^{m-1}\left(\frac{r_q}{a}\right)^m\cos(m\phi)\sin(\omega_{mnl}\tau) \tag{5}$$

$$W_{\phi,mnl}(\tau) = -2m\frac{ck_{mnl}}{\omega_{mnl}a}\left(\frac{r}{a}\right)^{m-1}\left(\frac{r_q}{a}\right)^m\sin(m\phi)\sin(\omega_{mnl}\tau) \tag{6}$$

$$\omega_{mnl}^2 = c^2\left(\left(\frac{u_{mn}}{R}\right)^2 + \left(\frac{l\pi}{h}\right)^2\right) \tag{7}$$

$\tau = s/c$, s is the distance between the exciting charge and a test charge, r_q is the transverse coordinate of the exciting charge and c is the velocity of light in vacuum. For a Gaussian bunch of charge q and bunch length σ_t ($\sigma_z = c\sigma_t$), one can calculate the integrated wakefield started from delta wakefield functions:

$$W_{G,z}(\tau) = \int_{-\infty}^{\tau} W_z(\tau - t)I(t)dt \tag{8}$$

$$W_{G,r}(\tau) = \int_{-\infty}^{\tau} W_r(\tau - t)I(t)dt \tag{9}$$

$$W_{G,\phi}(\tau) = \int_{-\infty}^{\tau} W_\phi(\tau - t)I(t)dt \tag{10}$$

where

$$I(t) = \frac{q}{(2\pi)^{1/2}\sigma_t}\exp\left(-\frac{t^2}{2\sigma_t^2}\right) \tag{11}$$

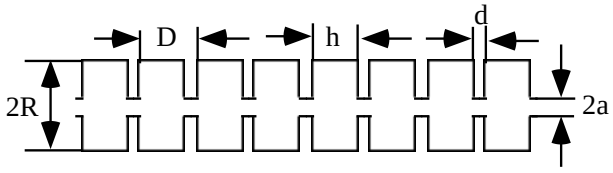

Figure 1: Disk-loaded accelerating structure

For the mth mode the total loss factor of a Gaussian bunch is:

$$K_m(\sigma_t) = \sum_{n=1}^{\infty}\sum_{l=0}^{\infty} k_{mnl}\exp(-\omega_{mnl}^2\sigma_t^2) \tag{12}$$

The general expression of the loss factor k_{mnl} corresponding to the mnlth pass-band is:

$$k_{mnl} = \frac{2\xi h u_{mn}^2 J_m^2\left(\frac{u_{mn}}{R}a\right)}{\left(\left(\frac{u_{mn}}{R}\right)^2+\left(\frac{l\pi}{h}\right)^2\right)\epsilon_0 D\pi R^4 J_{m+1}^2(u_{mn})}\left(\frac{S(x_1)^2+S(x_2)^2}{4}\right) \tag{13}$$

where

$$\xi = \begin{cases}1, m\neq 0\\ 1/2, m=0\end{cases} \tag{14}$$

$$S(x) = \frac{\sin(x)}{x} \tag{15}$$

and

$$x_1 = \frac{h}{2}\left(\left(\left(\frac{u_{mn}}{R}\right)^2+\left(\frac{l\pi}{h}\right)^2\right)^{1/2} - \frac{l\pi}{h}\right) \tag{16}$$

$$x_2 = \frac{h}{2}\left(\left(\left(\frac{u_{mn}}{R}\right)^2+\left(\frac{l\pi}{h}\right)^2\right)^{1/2} + \frac{l\pi}{h}\right) \tag{17}$$

2 Single bunch emittance growth in X and S bands linacs of NLC

In ref. 2 the single bunch transverse emittance blow up in a linac having a large number of accelerating sections has been studied by solving Langevin or Fokker-Planck equations, and the normalized emittance blow up can be expressed as:

$$\epsilon_{n,rms} = \frac{\sigma_y^2 l_s}{2\gamma(0)Gk(s,z)}\left(\frac{e^2 N_e W_\perp(0)}{m_0c^2}\right)^2 \tag{18}$$

where σ_y is the structure misalignment, l_s is the structure length, N_e is the particle population inside the bunch, $W_\perp(0)$ (V/C/m^2) is the transverse wakefield at the center of the bunch, m_0c^2 is the rest energy of the particle, $\gamma(0)G = eE_z/m_0c^2$, E_z is the effective accelerating gradient, and $k \approx 1/\beta_y$, where β_y is the average vertical beta function at the end of linac.

2.1 S-band linac

Taking NLC parameters: $\sigma_z = 0.0005$m, $l_s = 4$ m, $\gamma(0) = 2$ GeV/0.511 MeV=3.9×10^3, $\overline{k} = 1/20(m)$, $N_e = 1.1 \times 10^{10}$, $W_\perp(0) = 233V/pC/m^2$, and $G = \frac{17(MeV/m)}{2(GeV)} = 8.5 \times 10^{-3}$, one finds $\epsilon_{n,rms} = 7.6\sigma_y^2$. If one takes $\sigma_y = 50\mu$m, one finds $\epsilon_{n,rms} = 1.9 \times 10^{-8}$mrad. Comparing with the norminal vertical emittance at IP (14×10^{-8}mrad), one gets 1.4% emittance increase. Figs. 2, 3, and 4 show the loss factor spectra, short range wakefields and long range wakefields, respectively.

2.2 X-band linac

Taking NLC parameters: $\sigma_z = 0.000145$m, $\sigma_y = 14\mu$m, $l_s = 1.8$ m, $\gamma(0) = 10$ GeV/0.511 MeV=1.96×10^4, $\overline{k} = 1/30(m)$, $N_e = 1.1 \times 10^{10}$, $W_\perp(0) = 10^4 V/pC/m^2$, and $G = 54(MeV/m)/10(GeV) = 5.4 \times 10^{-3}$, one finds $\epsilon_{n,rms} = 300\sigma_y^2 = 5.9 \times 10^{-8}$mrad. Comparing with the norminal vertical emittance at IP (14×10^{-8}mrad), one gets 40% emittance increasing. Figs. 5, 6, and 7 show the loss factor spectra, short range wakefields and long range wakefields, respectively.

3 Multibunch beam dynamics in X and S bands linacs of NLC

In ref. 3 a criterion has been given to prevent the start up of multi-bunch instability in a detuned and damped linac. The loaded quality factor of the dipole mode and the wakefield reduction factor after one bunch seperation due to detuning effect has been established as follows:

$$Q_{1,L} < \frac{u_{11} s_b}{2Rln\left(\frac{4\pi e N_e R k_{110} \overline{\beta_y} \exp\left(-\frac{u_{11}^2 \sigma_z^2}{2R^2}\right) F(s_b)}{E_z u_{11} a^2}\right)} \tag{19}$$

where u_{11} is the first root of the Bessel function J_1, s_b is the bunch seperation in meter, R is the structure outer radius, σ_z is the bunch length, and $F(s_b)$ is the wakefield reduction factor after one bunch seperation.

Taking the parameters for S-band and X-band linacs one gets from eq. 19 two corresponding Q_{1L} vs F relations as shown in figs. 8 and 9.

4 HOM coupler design in S-band structure

In this section we discuss the HOM coupler design for the NLC S-band structure, and a general description on this kind of problem is given in ref. 4. Different

from X-band structure, the detuned S-band structure might be loaded with a few seperate HOM couplers [5]. To estimate the effect of each seperated HOM coupler it is interesting to start with a single pill-box cavity loaded by four waveguides as shown in Fig. 10 to damp TM_{110} mode. The loaded TM_{110} mode quality factor $Q_{L,110}$ can be calculated as follows:

$$Q_{L,110} = \frac{Q_{0,110}}{1+\beta_{4,110}} \tag{20}$$

where $Q_{0,110}$ is the unloaded quality factor and $\beta_{4,110}$ can be expressed as [4]:

$$\beta_{4,110}(l) = \frac{\pi Z_0 k k_{10} l^6 e^{-2\alpha_c t} J_1'(u_{11})^2}{144(ln(\frac{4l}{w})-1)^2 ABRR_{s,110}(R+h)J_2^2(u_{11})} \tag{21}$$

where h is the cavity length, R is the cavity radius, $R_{s,110}$ is the metal surface resistance at the TM_{110} mode frequency, λ_{110} is the wavelength of the TM_{110} mode, $Z_0 = 120\pi$, $k = 2\pi/\lambda_{110}$, $k_{10} = k(1-(\lambda_{110}/2A)^2)^{1/2}$, $\alpha_c = (2\pi/\lambda_{110})((\lambda_{110}/2l)^2-1)^{1/2}$, A and B are the width and the height of HOM waveguides, l and w are the width and the height of the four rectangular coupling slots with l parallel to the magnetic field, and t is the wall thickness between the cavity inner surface and the waveguide. As an example, taking $A = 0.044$ m, $B = 0.02$m, $w = 0.01$ m, $t = 0.003$ m, $h = 0.029$ m, and $R = 0.041$ m, one gets $\beta_{4,110}$ vs l as shown in Fig. 11. To estimate the effect of this HOM coupler cavity on N structure cavities, one can make the following rough estimations if the coupling between these N cavities is large enough:

$$Q_{L,N} = \frac{N}{(N-1)/Q_{0,110} + 1/Q_{L,110}} \tag{22}$$

For example, taking $N = 10$, $Q_{0,110} = 15000$, and $Q_{L,110} = 100$, one gets $Q_{L,N} = 943$.

5 Beam dynamics at IP region of NLC

The beam dynamics at IP region turns out to be a subject of study [6]. The cone shaped IP region of NLC [7] is simplified as shown in Fig. 12. The loss factor spectra, short and long range wakefields are shown in Figs. 13, 14 and 15 with bunch length of $\sigma_z = 145$ μm. Considering first single bunch dynamics, one has the differential equation of the transverse motion of a bunch with zero transverse dimension expressed as:

$$\begin{aligned} &\frac{d^2y(s,z)}{ds^2} + \frac{1}{\gamma(s,z)}\frac{d\gamma(s,z)}{ds}\frac{dy(s,z)}{ds} + k(s,z)^2 y(s,z) \\ &= \frac{1}{m_0c^2\gamma(s)} e^2 N_e \int_z^\infty \rho(z')\mathcal{W}_\perp(s,z'-z)y(s,z')dz' \end{aligned} \tag{23}$$

where $\int_{-\infty}^{\infty} \rho(z')dz' = 1$, z denotes the particle longitudinal position inside the bunch. Neglecting energy variation and the focusing effect, eq. 23 can be simplified as

$$\frac{d^2y(s,z)}{ds^2} = \frac{1}{m_0c^2\gamma(s)}e^2N_eW_\perp(z)y(s,z) \tag{24}$$

where $W_r(z) = W_\perp y$ is shown in Fig. 14d at $y = 0.014$m. Taking the maximum transverse wakefield at the tail ($5\sigma_z$), one finds the transverse offset between the head (- $5\sigma_z$) and the tail ($5\sigma_z$) is 16 nm. To remind the reader the bunch transverse dimensions at IP are σ_y/σ_x =7.7 nm/422 nm. The maximum tail particle angle variation is about 14 nrad which is very small compared with $\sigma_x/\sigma_z = 2.9 \times 10^{-3}$ rad. The additional single bunch energy variation within the bunch due to IP cavity like region is about 0.1 MeV. Concerning multi-bunch instabilities, one can make numerical simulations started from the long range wakefields given in Fig. 15.

6 Conclusions

1) NLC X-band and S-band wakefields have been calculated.
2) Long range and short range wakefields in IP region volume have been evaluated.
3) Single bunch emittance blow-up in S-band and X-band main linacs have been estimated by analytical formula. It is found that with 50μm S-band structure misaligment there is 1.4% emittance increase, and with 14μm X-band structure misaligment there is 42% emittance growth.
4) Transverse multi-bunch instabilities in S-band and X-band main linacs of NLC have been studied. Two relations of dipole mode loaded Q_{1L} factors vs wakefield detuning reduction factors, F, are found for two linacs. X-band: $Q_{1L} < 146/ln(600F)$, and S-band: $Q_{1L} < 40/ln(17F)$. We understand that these limits might be somewhat tighter than reality.
5) Single bunch transverse deflection and bunch length variation due to IP cavity like region are about 16 nm in the horizontal and 1.46 μm, respectively. The additional energy variation is about 0.1 MeV.
6) Multi-bunch instabilities in the IP region can be neglected.

7 Acknowledgements

I thank very much the invitation from R. Ruth to visit SLAC working on NLC project. I have enjoyed fruitful discussions with Tor Raubenheimer who initiated the investigation on the beam dynamics in the IP region and made many comments on this report. The warm hospitalities from SLAC and colleagues are appreciated. I thank K. Ko for kindly providing me his office during the visit. I appreciate the discussions with K. Bane, A. Chao, S. Heifets, R. Jones, K. Ko,

N. Kroll, Z. Li, E. Lin, B. McCandless, M. Minty, Cho. Ng, G. Stupakov, S. Tzenov, J.W. Wang, D. Whittum, and many others.

References

[1] J. Gao, "Analytical formulae for the loss factors and wakefields of a disk-loaded accelerating structure", *Nucl. Instr. and Methods*, **A381** (1996), p. 174.

[2] J. Gao, "Analytical treatment of the emittance growth in the main linacs of future linear colliders", LAL-SERA-99-82, 1999.

[3] J. Gao, "Theoretical investigation on multibunch instabilities in electron storage rings and linear accelerators", PAC97, Vancouver, Canada, May 1997, p. 1608.

[4] J. Gao, "On the higher order mode coupler design for damped accelerating structures", Proceedings of PAC95, p. 1717.

[5] Z. Li, private communications.

[6] T. Raubenheimer, private communications.

[7] http://www-project.slac.stanford.edu/nlc/home.html

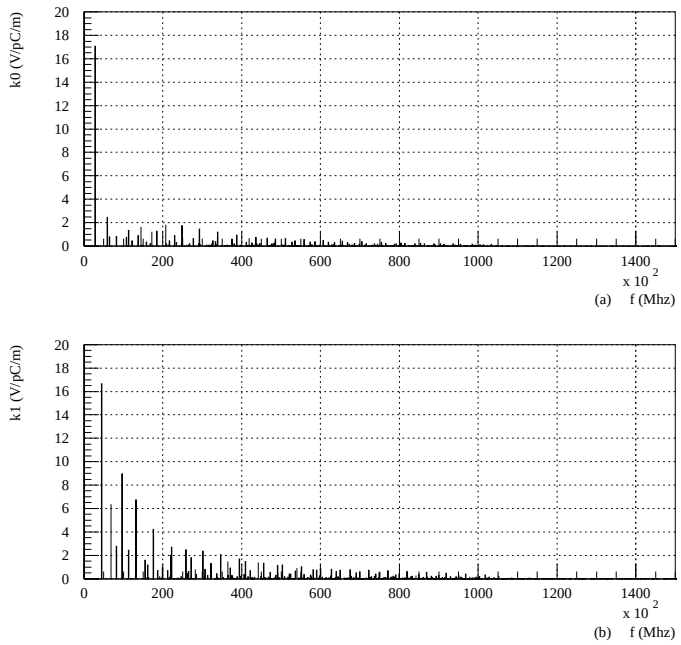

Figure 2: NLC S-Band linac: (a) The monopole mode loss factors vs frequencies, and (b) the dipole mode loss factors vs frequencies, with $a = 0.015$ m, $R = 0.041$ m, $D = 0.035$ m, $h = 0.029$ m, and $\sigma_z = 0.0005$ m.

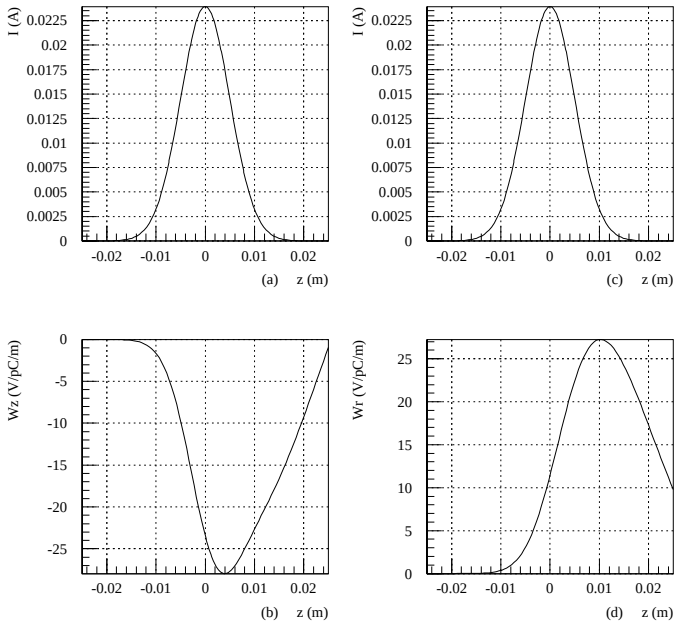

Figure 3: NLC S-Band linac: (a) and (b) are the bunch current distributions, (c) and (d) are the short range longitudinal and transverse wakefields, with $a = 0.015$ m, $R = 0.041$ m, $D = 0.035$ m, $h = 0.029$ m, and $\sigma_z = 0.0005$ m. The transverse wakefield is measured at $r = a$.

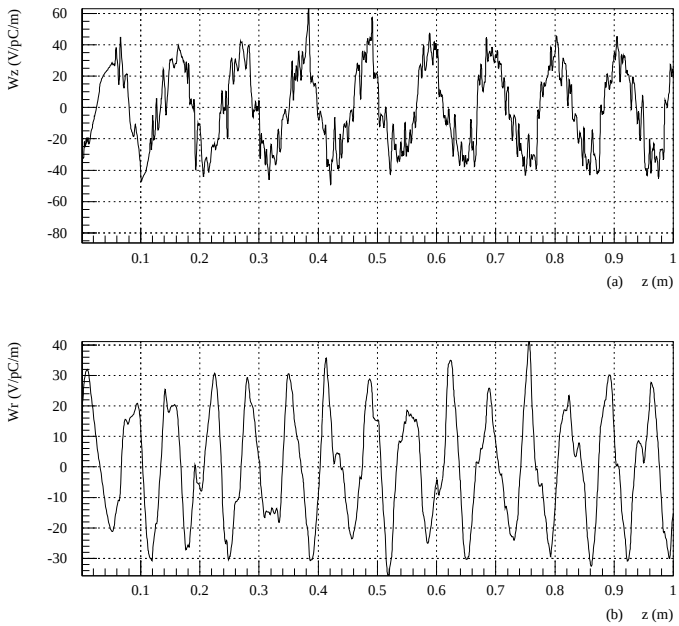

Figure 4: NLC S-Band linac: (a) The monopole mode long range wakefield, and (b) the dipole mode long range wakefield, with $a = 0.015$ m, $R = 0.041$ m, $D = 0.035$ m, $h = 0.029$ m, and $\sigma_z = 0.0005$ m. The transverse wakefield is measured at $r = a$.

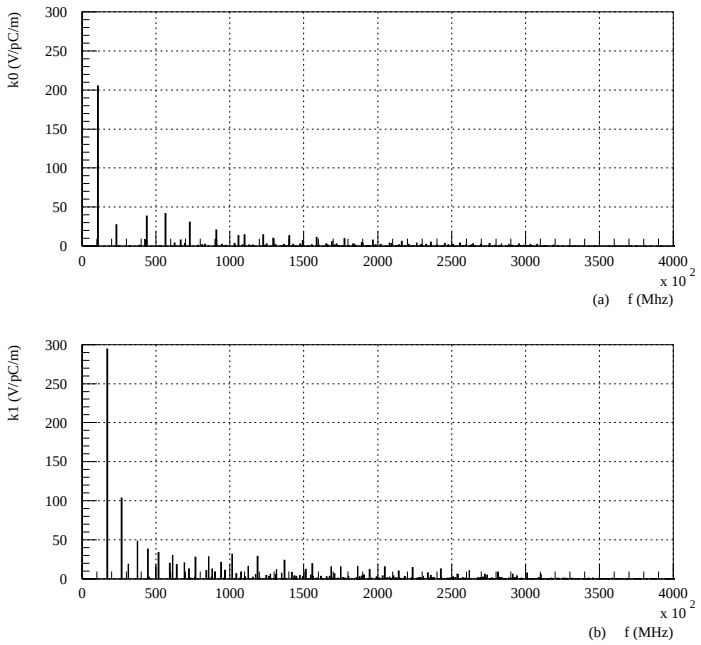

Figure 5: NLC X-Band linac (no. 102): (a) The monopole mode loss factors vs frequencies, and (b) the dipole mode loss factors vs frequencies, with $a = 0.0048$ m, $R = 0.0107$ m, $D = 0.008747$ m, $h = 0.00729$ m, and $\sigma_z = 0.000145$ m.

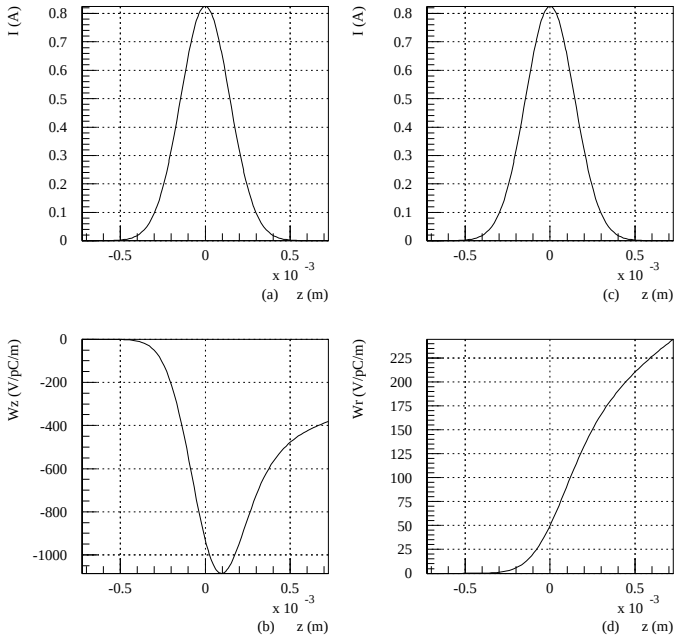

Figure 6: NLC X-Band linac (no. 102): (a) and (b) are the bunch current distributions, (c) and (d) are the short range longitudinal and transverse wakefields, with $a = 0.0048$ m, $R = 0.0107$ m, $D = 0.008747$ m, $h = 0.00729$ m, and $\sigma_z = 0.000145$ m. The transverse wakefield is measured at $r = a$.

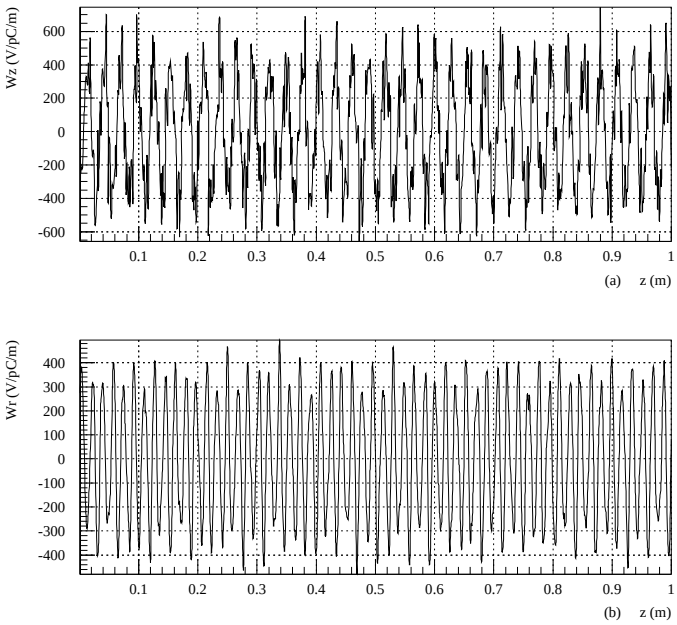

Figure 7: NLC X-Band linac (no. 102): (a) The monopole mode long range wakefield, and (b) the dipole mode long range wakefield, with $a = 0.015$ m, $R = 0.041$ m, $D = 0.035$ m, $h = 0.029$ m, and $\sigma_z = 0.0005$ m. The transverse wakefield is measured at $r = a$. (No detuning)

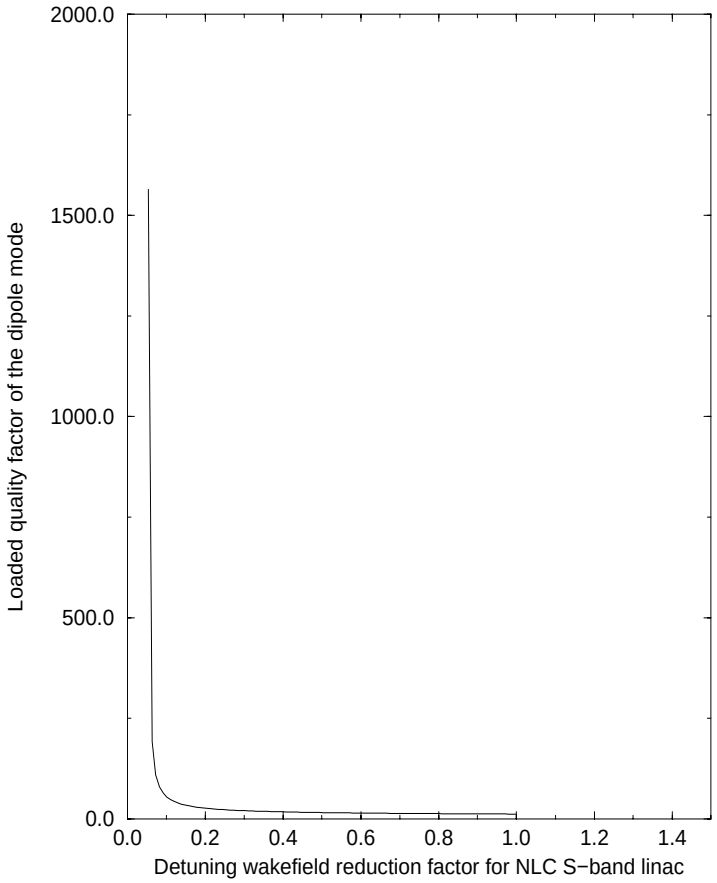

Figure 8: The loaded quality factor of the dipole mode vs the wakefield reduction factor, F, after one bunch seperation due to detuning effect of the S-band structure ($Q_{1L} < 40/ln(17F)$).

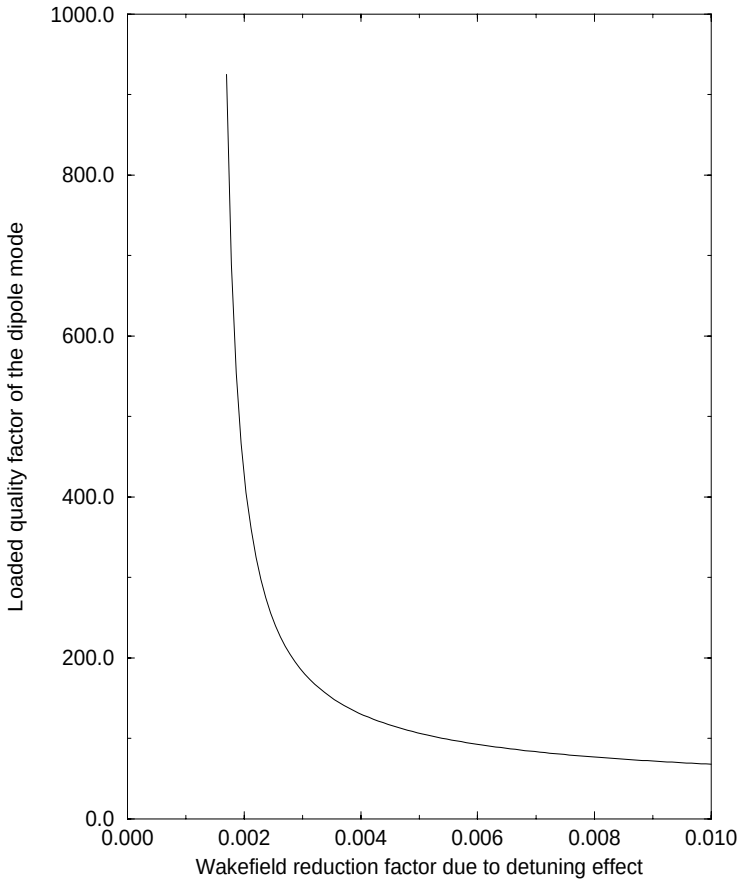

Figure 9: The loaded quality factor of the dipole mode vs the wakefield reduction factor, F, after one bunch seperation due to detuning effect of the X-band structure ($Q_{1L} < 146/ln(600F)$).

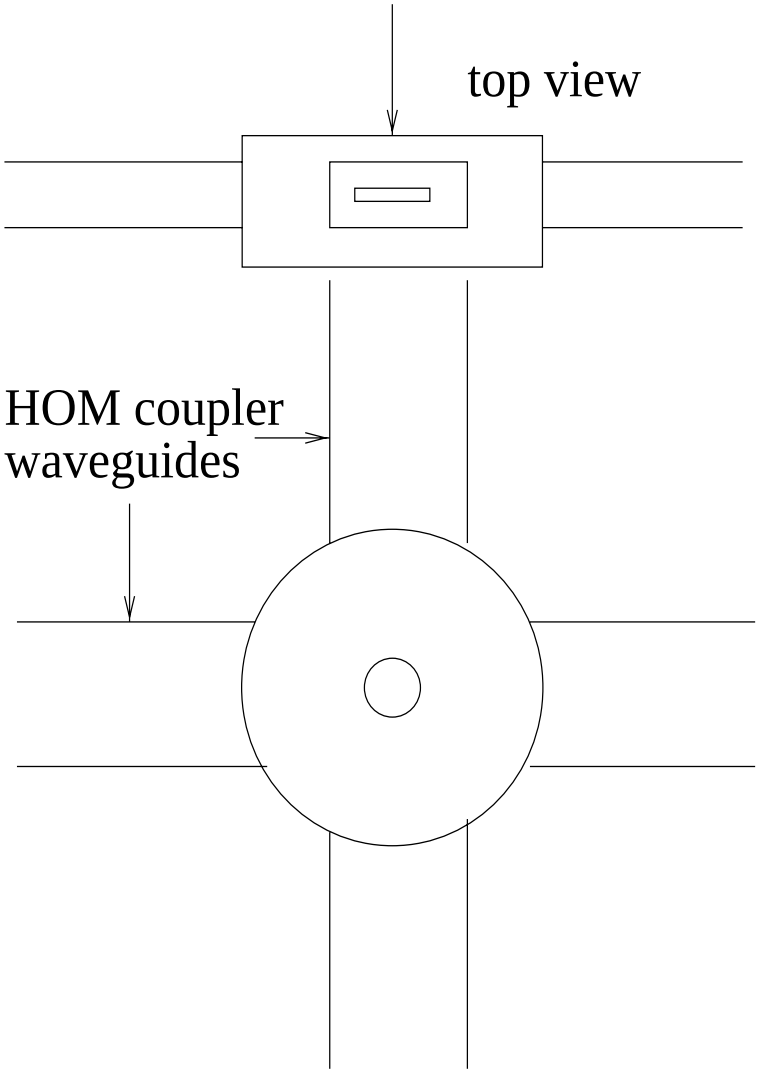

Figure 10: The schematical drawing of a single cavity lodaded by four HOM waveguides.

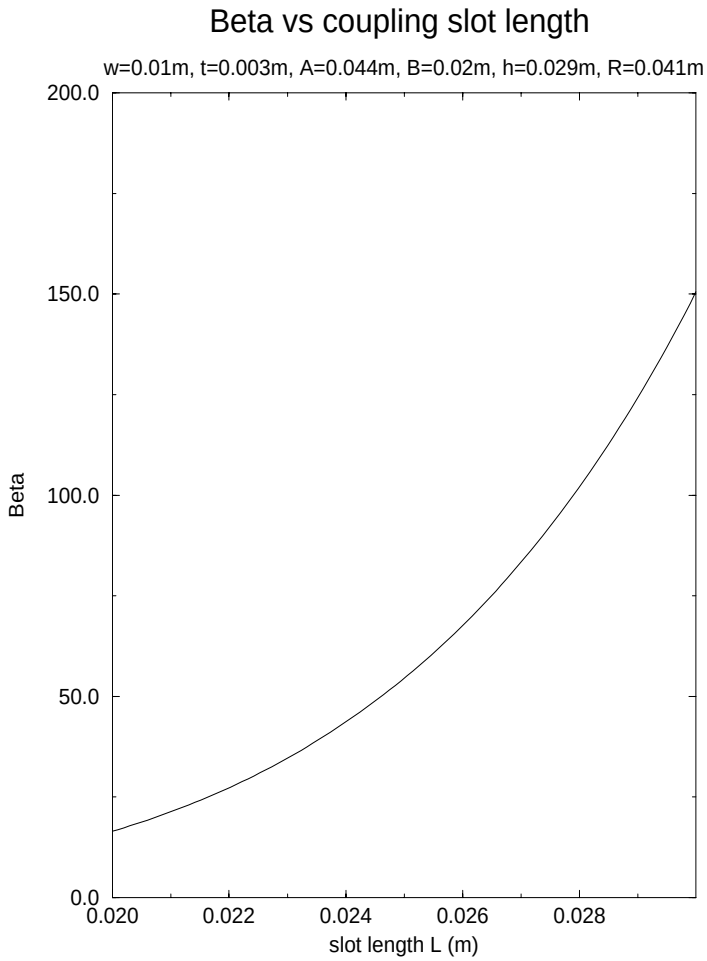

Figure 11: The coupling coefficient β vs the coupling slot length l.

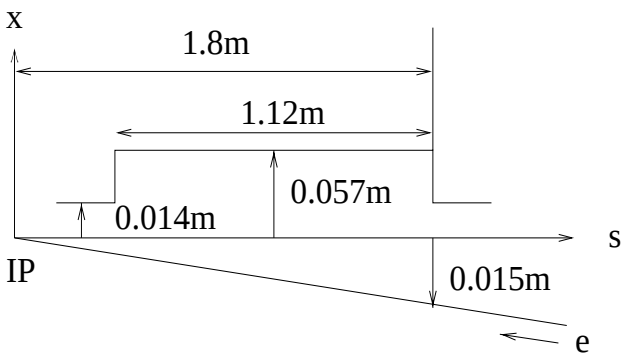

Figure 12: The simplified IP region.

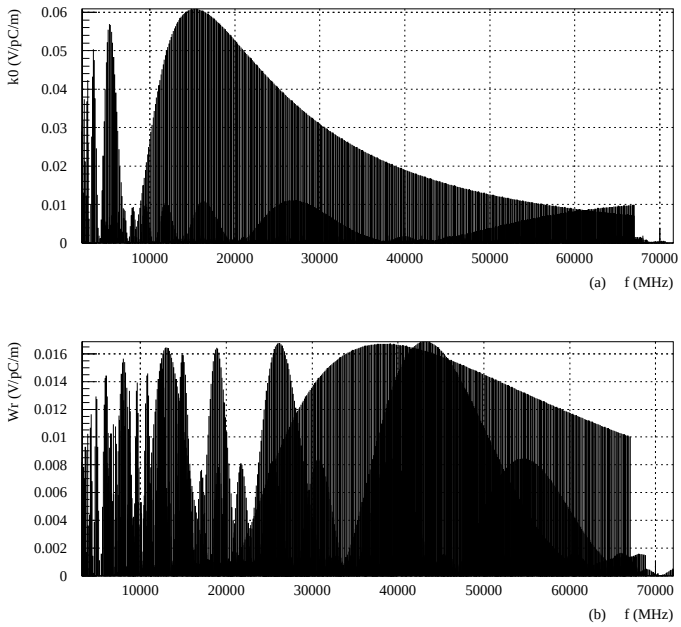

Figure 13: IP region cavity: (a) The monopole mode loss factors vs frequencies, and (b) the dipole mode loss factors vs frequencies, with $a = 0.014$ m, $R = 0.057$ m, $D = h = 1.12$ m, and $\sigma_z = 0.000145$ m.

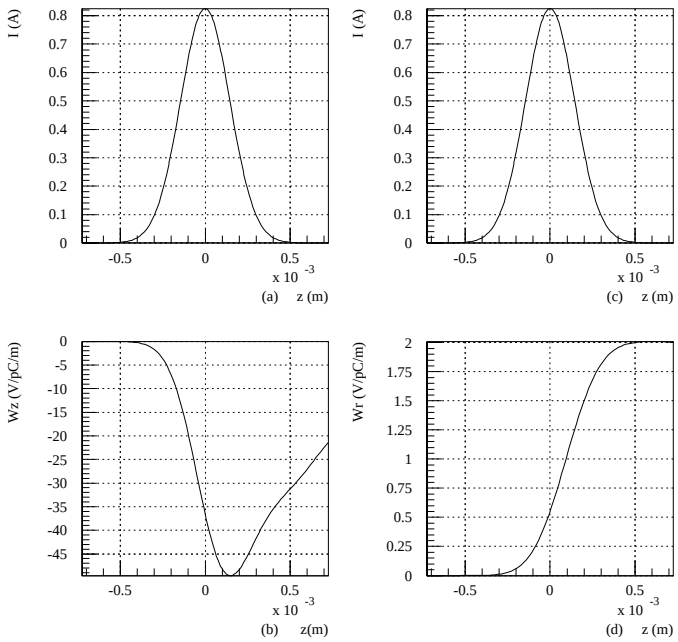

Figure 14: IP region cavity: (a) and (b) are the bunch current distributions, (c) and (d) are the short range longitudinal and transverse wakefields, with $a = 0.014$ m, $R = 0.057$ m, $D = h = 1.12$ m, and $\sigma_z = 0.000145$ m. The transverse wakefield is measured at $r = a$.

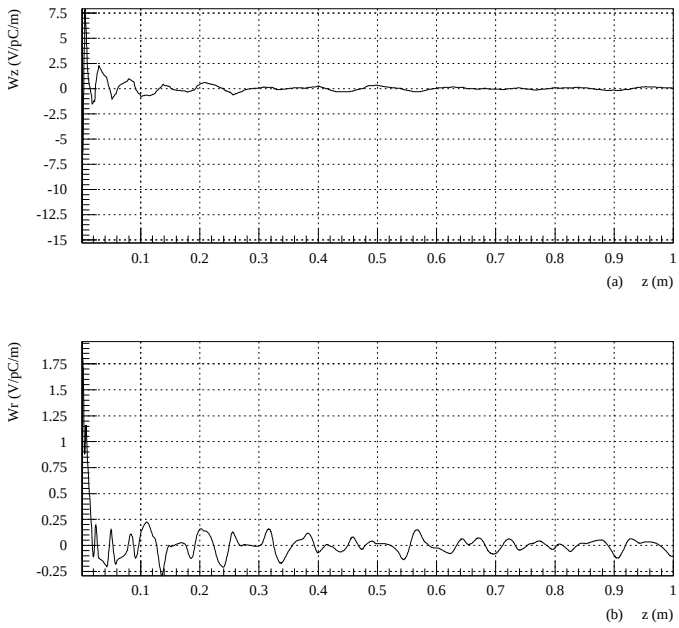

Figure 15: IP region cavity: (a) The monopole mode long range wakefield, and (b) the dipole mode long range wakefield, with $a = 0.014$ m, $R = 0.057$ m, $D = h = 1.12$ m, and $\sigma_z = 0.000145$ m. The transverse wakefield is measured at $r = a$.